

PII: S0017-9310(96)00347-X

Modeling of Darcy–Forchheimer drag for fluid flow across a bank of circular cylinders

S. L. LEE and J. H. YANG

Department of Power Mechanical Engineering, National Tsing-Hua University, Hsinchu 30043, Taiwan

(Received 22 February 1996 and in final form 27 September 1996)

Abstract—In the present investigation, an incompressible fluid flow across a bank of circular cylinders is studied and modeled as a non-Darcy flow through a porous medium. The continuity equation and the momentum equation in pore scale are solved on a Cartesian grid system. To circumvent the numerical difficulties arising from the flow domain of irregular shape, the weighting function scheme along with the APPLE algorithm and the SIS solver is employed. The Darcy–Forchheimer drag is then determined from the resulting volumetric flow rate under a prescribed pressure drop. The result indicates that the permeability approaches zero at the particular porosity of 0.2146 when the fluid flow across the cylinders becomes impossible. In addition, the pressure drag (Forchheimer drag) is found to contribute a significant resistance at large porosities and/or large granule Reynolds numbers. A correlation of Darcy–Forchheimer drag is proposed for $0.2146 \leq \varepsilon \leq 1$ and $0 \leq Re_d \leq 50$. © 1997 Elsevier Science Ltd.

INTRODUCTION

Fluid flow across a bank of circular cylinders is encountered in many scientific and engineering activities. For practical purpose, the bank of cylinders can be modeled as a porous medium under most situations [1]. However, few efforts have been devoted to such a modeling in the past. Nevertheless, there exists a voluminous literature dealing with modeling for particle-like or granular media.

Physically, the flow resistance in non-Darcy flow is expressible as the sum of a viscous friction and a pressure drag [2–5]. For convenience, the viscous friction, the pressure drag and their sum (the total drag) will be, respectively, referred to as the Darcy drag, the Forchheimer drag and the Darcy–Forchheimer drag in the present study. After examining a number of experimental data, Ergun [5] proposed a well-known correlation of Darcy–Forchheimer drag for beds of granular solids. The two coefficients employed in the correlation are constant ($\alpha = 150$ and $\beta = 1.75$) in spite of orientation, shape and surface of the granular solids. However, in a review paper Macdonald *et al.* [6] suggested $\alpha = 180$ and $\beta = 1.8$ – 4.0 depending on surface roughness of the particles for Ergun's correlation [5].

In 1964, Ward [7] proposed a similar correlation with a dimensionless constant c (i.e. $c = \beta\alpha^{-0.5}\varepsilon^{-1.5}$ according to Ergun's modeling [5]). He claimed that c has the same value ($c = 0.550$) for all porous media. The “universal” constant of $c = 0.550$ was subsequently verified by Beavers *et al.* [8] through an experiment on a randomly packed beds of spheres. However, in an experiment on non-Darcy flow through fibrous porous media, Beavers and Sparrow

[9] obtained a c -value of 0.074 that is far smaller than the aforementioned “universal constant” ($c = 0.550$). Even the free fiber ends were found to have a great influence on the c -value. This seems to substantiate the dependence of the Darcy–Forchheimer drag upon the microstructure of the porous medium. Hence, the existing models for beds of granular solids are not necessarily appropriate for other classes of porous media as remarked by Beavers and Sparrow [9].

To the authors' best knowledge, Coulaud *et al.* [10] might be the only attempt in the literature to model the Darcy–Forchheimer drag by using a numerical method. They computed the pressure drop for a fluid flow across a bank of circular cylinders at given flow rates (or granule Reynolds numbers Re_d) up to $Re_d = 25$. The resulting pressure drop was decomposed into three zones, namely, the Darcy zone ($Re_d \leq 1$), the transition zone ($1 \leq Re_d \leq 13$) and the Forchheimer zone ($Re_d \geq 13$). For each of the three porosities ($\varepsilon = 0.4345, 0.6073, 0.8076$) investigated by them, a permeability K was obtained for the Darcy zone, while the aforementioned coefficient c was found proportional to $K^{-1/2}$ in the Forchheimer zone rather than a constant. In the transition zone, however, no correlation was performed.

Generally speaking, significant departures from the Darcy's law would occur at granule Reynolds numbers on the order of one [9]. However, the Forchheimer drag obtained by Coulaud *et al.* [10] is seen to be negligibly small as compared to the Darcy drag even at a large granule Reynolds number. For instance, the Forchheimer drag predicted by Coulaud *et al.* [10] makes only 5% of the total drag for a granule Reynolds number as large as 20. Their underestimation on the Forchheimer drag is believed to

NOMENCLATURE

<p>a_{mn} coefficients of a bi-polynomial, equation (15)</p> <p>c a constant</p> <p>d diameter of the cylinders [m]</p> <p>F Forchheimer coefficient, equation (11)</p> <p>H width of a bank of circular cylinders [m]</p> <p>K permeability of porous media [m²]</p> <p>L pitch of cylinder bank [m]</p> <p>m, n indicies of a bi-polynomial, equation (15)</p> <p>P, p pressure [N m⁻²] and dimensionless pressure, $p = P/\Delta P$</p> <p>\bar{P} volume-averaged pressure [N m⁻²]</p> <p>q volumetric flow rate, equation (7)</p> <p>Re_c characteristic Reynolds number, $U_c L/\nu$</p> <p>Re_d granule Reynolds number, $\bar{U}d/\nu$</p> <p>U, V velocity components [m s⁻¹]</p> <p>\bar{U} superficial velocity [m s⁻¹], equation (8)</p> <p>U_c characteristic velocity, $\sqrt{\Delta P/\rho}$</p>	<p>u, v dimensionless velocities, $U/U_c, V/U_c$</p> <p>X, Y coordinates [m]</p> <p>X_0, Y_0 location of a unit cell, Fig. 1.</p> <p>Greek symbols</p> <p>α, β coefficients, equation (13)</p> <p>γ fraction of the Forchheimer drag, equation (14)</p> <p>ΔP a prescribed pressure drop [N m⁻²]</p> <p>$\Delta\psi$ increment of the streamlines, $\psi_{\max}/10$</p> <p>$\Delta\xi, \Delta\eta$ mesh of the Cartesian grid system</p> <p>ε porosity, equation (10)</p> <p>ε_{\min} minimum possible porosity</p> <p>μ dynamic viscosity [kg m⁻¹ s⁻¹]</p> <p>ν kinematic viscosity [m² s⁻¹]</p> <p>ρ density of the fluid [kg m⁻³]</p> <p>ψ stream function, equation (6)</p> <p>ξ, η dimensionless local coordinates.</p> <p>Subscript</p> <p>max maximum.</p>
--	---

arise from an improper methodology and a coarse grid system used by them.

The purpose of this paper is to propose a numerical procedure for modeling the Darcy–Forchheimer drag. The continuity equation and the momentum equation in pore scale are solved numerically for an incompressible fluid flow across a bank of circular cylinders at a prescribed pressure drop. The Darcy–Forchheimer drag is then determined from the corresponding volumetric flowing rate. A correlation for the Darcy–Forchheimer drag is performed for all of the possible porosities ($0.2146 \leq \varepsilon \leq 1$) with a granule Reynolds number up to 50. Comparisons with the numerical model from Coulaud *et al.* [10] will be discussed.

THEORETICAL ANALYSIS

Consider a fluid flow across a bank of circular cylinders of diameter d . The cylinders are staggered with row (column) spacing L as shown in Fig. 1. The diameter of the cylinder is very small as compared to the width of the bank of the cylinders ($d \ll H$). Therefore, the flow can be assumed incompressible and laminar through each “channel” formed by two adjacent rows of cylinders as long as the granule Reynolds number Re_d is not large. Furthermore, it can be treated as a periodic flow with a constant pressure drop ΔP after each period L in the “fully developed” region. This implies that only the flow inside a unit cell (i.e. $X_0 \leq X \leq (X_0 + L)$ and $Y_0 \leq Y \leq (Y_0 + L)$) is needed to solve. After imposing the assumptions, the governing equations are expressible as

$$\frac{\partial u}{\partial \xi} + \frac{\partial v}{\partial \eta} = 0 \quad (1)$$

$$u \frac{\partial u}{\partial \xi} + v \frac{\partial u}{\partial \eta} = -\frac{\partial p}{\partial \xi} + \frac{1}{Re_c} \left(\frac{\partial^2 u}{\partial \xi^2} + \frac{\partial^2 u}{\partial \eta^2} \right) \quad (2)$$

$$u \frac{\partial v}{\partial \xi} + v \frac{\partial v}{\partial \eta} = -\frac{\partial p}{\partial \eta} + \frac{1}{Re_c} \left(\frac{\partial^2 v}{\partial \xi^2} + \frac{\partial^2 v}{\partial \eta^2} \right) \quad (3)$$

where the dimensionless variables are defined by

$$\begin{aligned} u &= U/U_c & v &= V/U_c & \xi &= (X - X_0)/L \\ \eta &= (Y - Y_0)/L & p &= P/\Delta P & U_c &= \sqrt{\Delta P/\rho} \\ Re_c &= U_c L/\nu. \end{aligned} \quad (4)$$

The associated boundary conditions are

$$\begin{aligned} u(0, \eta) &= u(1, 1 - \eta) & v(0, \eta) &= v(1, 1 - \eta) \\ p(0, \eta) &= p(1, 1 - \eta) + 1 & \partial u(\xi, 0)/\partial \eta &= 0 \\ \partial v(\xi, 0)/\partial \eta &= 0 & \partial p(\xi, 0)/\partial \eta &= 0 & \partial u(\xi, 1)/\partial \eta &= 0 \\ \partial v(\xi, 1)/\partial \eta &= 0, & \partial p(\xi, 1)/\partial \eta &= 0. \end{aligned} \quad (5)$$

Note that the no-slip condition should be imposed on the surface of the cylinders. Thus, there is no need to solve the governing equations inside the cylinders.

The governing equations (1)–(3) and the associated boundary conditions (5) constitute a system of partial differential equations on a physical domain of irregular shape. Such a problem can be efficiently solved by using the weighting function scheme [11–12] along with the APPLE algorithm [13] and the SIS solver [14] on a Cartesian grid system as shown in Fig. 2. In

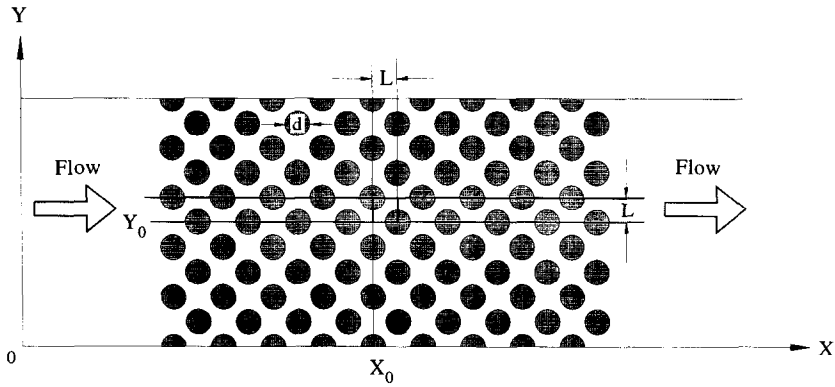


Fig. 1. Fluid flow across a bank of circular cylinders.

the present study, the primary variables (u, v, p) are obtained for each prescribed value of $(Re_c, d/L)$. The numerical procedure is iterated until the solution (u, v, p) converges within a tolerance of 10^{-5} , while the dilation $(\partial u/\partial x + \partial v/\partial y)$ of the velocity has a magnitude of less than 10^{-4} . The grid mesh $\Delta\xi = \Delta\eta = 0.02$ was found adequate for all of the parameters under study. Further reduction in the grid size does not show significant influence on the solution.

Once the velocity is known, the dimensionless stream function ψ can be evaluated from

$$\psi = \int_0^\eta u \, d\eta. \tag{6}$$

It appears that the stream function reaches a maximum known as the dimensionless volumetric flow rate

$$q = \psi_{\max} = \int_0^1 u \, d\eta \tag{7}$$

at $\eta = 1$. Note also that the volumetric flow rate of q

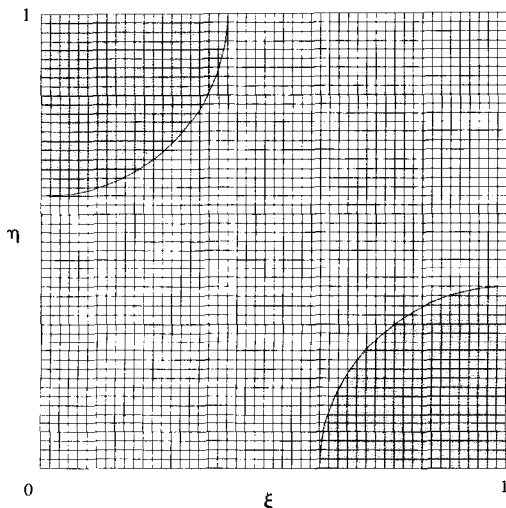


Fig. 2. The Cartesian grid system employed in the present study for a unit cell.

should be independent of the position ξ . The variation of q upon ξ in the present numerical results is found less than 0.01%. This is a proof of the effectiveness and the correctness of the present computations. Based on this, the superficial velocity \bar{U} and the granule Reynolds number Re_d are evaluated from

$$\bar{U} = \frac{1}{L} \int_{Y_0}^{Y_0+L} U \, dY = U_c q \tag{8}$$

$$Re_d = \frac{\bar{U}d}{\nu} = Re_c \left(\frac{d}{L}\right) q. \tag{9}$$

Figure 3 reveals the results of streamlines and isobars for $d/L = 0.8$ at the prescribed Reynolds numbers of $Re_c = 1, 10$ and 30 . To achieve an existence and a uniqueness for the pressure solution, a pressure level has been defined by $p(1, 1) = 0$ through the use of the APPLE algorithm [13]. For convenience, the results are presented on two adjacent unit cells, while the increment of the streamlines is assigned by $\Delta\psi = \psi_{\max}/10$.

From Fig. 3(a), it is seen that both streamlines and isobars at $Re_c = 1$ (corresponding to $Re_d = 0.02176$) are essentially symmetric about the vertical line $\xi = 1$. This means that the viscous friction dominates the drag force under such a low Reynolds number. When the Reynolds number increases to $Re_c = 10$ or $Re_d = 2.176$, the streamlines and isobars show a slight deviation from symmetry as revealed by Fig. 3(b). Finally, an asymmetric flow can be found from Fig. 3(c) when the granule Reynolds number Re_d is as large as 15.72 ($Re_c = 30$). It is important to note from Fig. 3(c) that as the Reynolds number is sufficiently large, a pressure drag could arise from the asymmetric pressure distribution on the cylinder surface.

MODELING OF THE DARCY-FORCHHEIMER DRAG

In most applications, there is no need to solve the fluid flow in pore scale for a problem like that in the previous section. Modeling the cylinders as a porous medium and solving only the volume-averaged flow

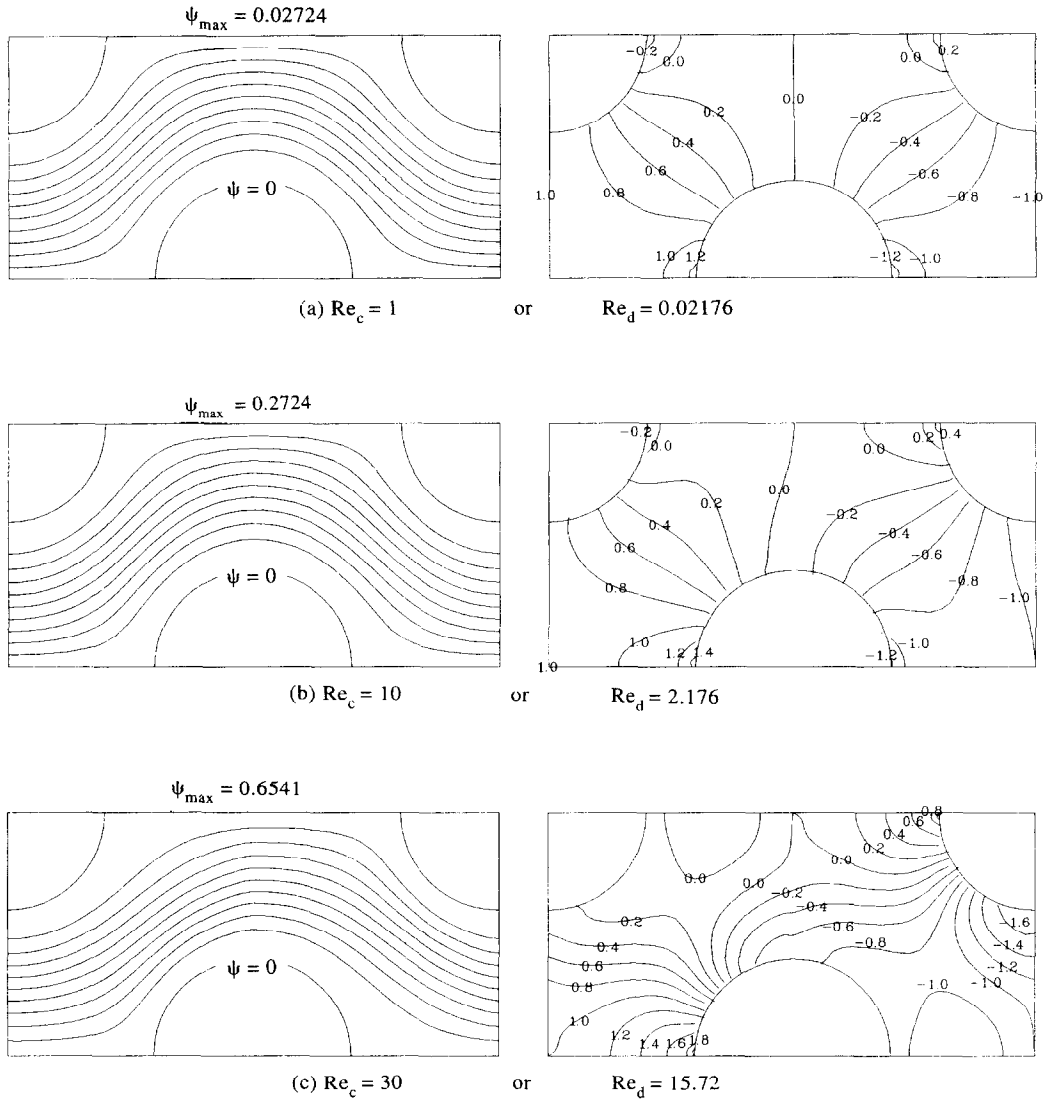


Fig. 3. Streamlines (increment $\Delta\psi = \psi_{\max}/10$) and isobars for the cases of $d/L = 0.8$ and (a) $Re_c = 1$; (b) $Re_c = 10$; and (c) $Re_c = 30$.

quantities would be practically enough. As suggested by Reynolds [2], Forchheimer [3], Blake [4] and Ergun [5], the porosity ε and the average pressure gradient $(-d\bar{P}/dX)$ for the fluid flow across a bank of circular cylinders as shown in Fig. 1 are assumed the form

$$\varepsilon = 1 - \left(\frac{\pi}{8}\right)\left(\frac{d}{L}\right)^2 \tag{10}$$

$$-\frac{d\bar{P}}{dX} = \frac{\Delta P}{L} = \left(\frac{d^2}{K} + FRe_d\right)\frac{\mu\bar{U}}{d^2} \tag{11}$$

where K is known as the permeability of the porous medium and F is the Forchheimer coefficient. The dimensionless quantities (d^2/K) , (FRe_d) and $(d^2/K + FRe_d)$ are respectively the Darcy drag, the Forchheimer drag and the Darcy-Forchheimer drag.

For the problem studied in the previous section, the

volumetric flow rate q can be determined for each assigned value of $(Re_c, d/L)$. Thus, the Darcy-Forchheimer drag can be evaluated from

$$\frac{d^2}{K} + FRe_d = \frac{\Delta P d^2}{L\mu\bar{U}} = Re_c \left(\frac{d}{L}\right)^2 \frac{1}{q} \tag{12}$$

once q is known. Figure 4 shows the results of the Darcy-Forchheimer drag vs the granule Reynolds number Re_d (up to 50) at various porosity ε . Note that for $Re_d < 150$ the fluid flow across a single cylinder is laminar [15]. Hence, the fluid flow across a bank of circular cylinders is believed to be laminar also for $Re_d \leq 50$.

As observable from the ordinate of Fig. 4, the Darcy-Forchheimer drag reduces to d^2/K when the viscous friction dominates the drag force ($Re_d \cong 0$). In contrast, the pressure drag (i.e. the Forchheimer

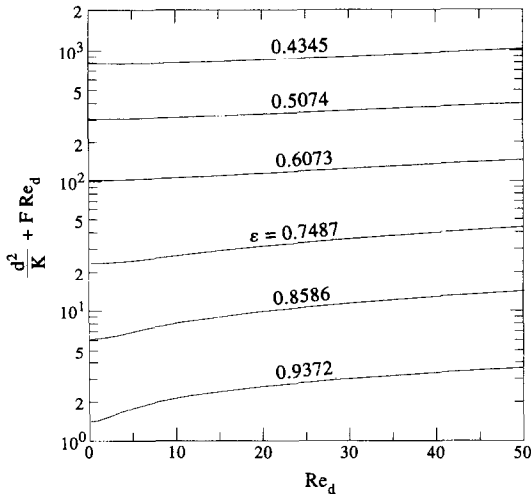


Fig. 4. Present results of Darcy–Forchheimer drag at various porosities ϵ and granule Reynolds numbers Re_d .

drag) could overtake the viscous friction and become the leading drag force as the granule Reynolds number Re_d is sufficiently large. This is especially true when the porosity ϵ is large. For instance, at $\epsilon = 0.9372$ (i.e. $d/L = 0.4$) the Forchheimer drag ($F Re_d$) increases from zero to 2.621 as Re_d increases from zero to 50, while the Darcy drag is maintained at $d^2/K = 1.427$. Under this situation, using the Darcy law would lead to a significant error. In case of small porosity, say $\epsilon = 0.4345$ ($d/L = 1.2$), the Darcy drag would essentially dominate the drag for a wide range of granule Reynolds numbers. These findings are consistent with the physical reasoning.

In his well-known investigation, Ergun [5] proposed a simple correlation for the Darcy–Forchheimer drag

$$\frac{d^2}{K} + F Re_d = \alpha \frac{(1-\epsilon)^2}{\epsilon^3} + \beta \frac{(1-\epsilon)}{\epsilon^3} Re_d \quad (13)$$

based on a number of experiments of fluid flow through beds of granular solids. If the same form of correlation (13) is adopted for the present result dealing with a flow across a bank of circular cylinders, however, α would be a function of ϵ rather than a constant. To clarify this point, the function $\alpha(\epsilon)$ converted from the result shown in Fig. 4 is revealed in Fig. 5. The α -value ($\alpha = 150$) from Ergun [5] and that from Coulaud *et al.* [10] are also presented in Fig. 5 for comparison.

It is interesting to note from Fig. 5 that the present result of $\alpha(\epsilon)$ agrees excellently with that from Ergun [5] in a range of ϵ ($0.6 \leq \epsilon \leq 0.7$). Otherwise, a direct application of Ergun’s correlation on a fluid flow across a bank of cylinders would always underestimate the Darcy drag (d^2/K). Note also that the minimum possible ϵ for cylinder bundle is $\epsilon_{\min} = 0.2146$ ($d/L = \sqrt{2}$) when the cylinders contact with each other. Under such a situation, flow across the cylinders becomes theoretically impossible and thus possesses an α -value of infinity.

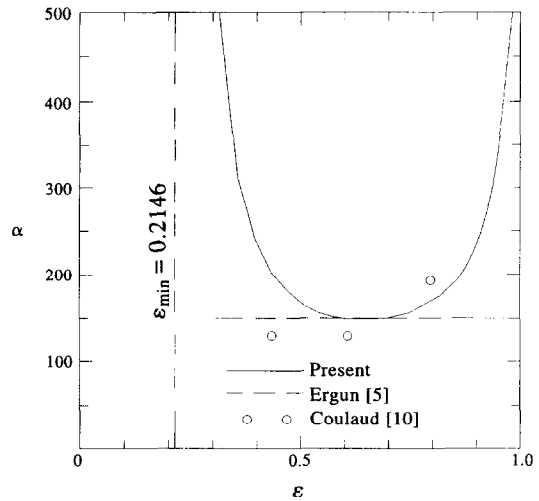


Fig. 5. Comparison of $\alpha(\epsilon)$ among the present result and that from Coulaud *et al.* [10] and Ergun [5].

result seems to successfully reflect this particular physical phenomenon. The numerical result from Coulaud *et al.* [10], however, does not predict such an infinite α -value.

A comparison between the Darcy–Forchheimer drag from Coulaud *et al.* [10] and that from the present study is depicted in Fig. 6. Ergun’s correlation for beds of granular particles is also plotted in Fig. 6 as a reference. For convenience, the available results of $(d^2/K, F Re_d)$ and the corresponding fraction of the Forchheimer drag

$$\gamma = F Re_d / (d^2/K + F Re_d) \quad (14)$$

are listed in Table 1 for the three porosities $\epsilon = 0.4345, 0.6073, 0.8076$ at $Re_d = 20$. From Fig. 6 and Table 1, Coulaud *et al.* [10] are seen to greatly underestimate the Forchheimer drag. For instance, at $(Re_d, \epsilon) = (20, 0.6073)$ their result predicts that the

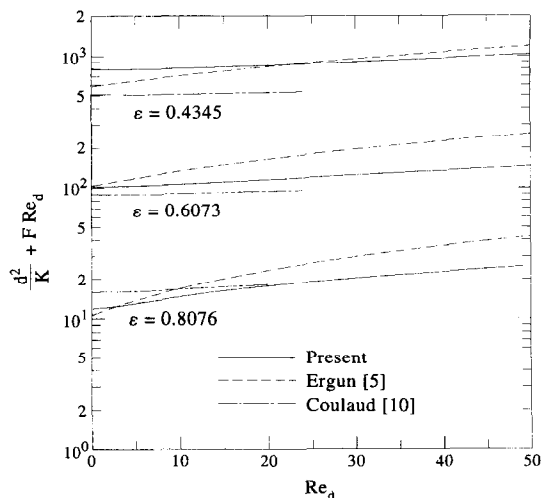


Fig. 6. Comparison of the Darcy–Forchheimer drag among the present result and that from Coulaud *et al.* [10] and Ergun [5] for $\epsilon = 0.4345, 0.6073$ and 0.8076 .

Table 1. Comparison of $(d^2/K, F Re_d, \gamma)$ among the available models for $Re_d = 20$

ε	Model	d^2/K	$F Re_d$	γ
0.4345	Present ^a	787.95	55.60	6.59%
	Coulaud [10] ^a	505.58	18.96	3.61%
	Ergun [5] ^b	584.77	241.29	29.21%
0.6073	Present ^a	102.20	12.83	11.15%
	Coulaud [10] ^a	89.09	5.17	5.48%
	Ergun [5] ^b	103.28	68.32	39.81%
0.8076	Present ^a	11.85	5.86	33.09%
	Coulaud [10] ^a	15.85	2.22	12.29%
	Ergun [5] ^b	10.54	12.78	54.80%

(a) Flow across cylinder bundle.
(b) Flow through granular beds.

Forchheimer drag makes only 5.48% of the total drag. Such a fraction of Forchheimer drag is incredibly low as compared to 11.15% from the present result. It is noted that Ergun's correlation [5] gives a fraction of Forchheimer drag as large as 39.81% for granular beds under the same parameters.

In their work, Coulaud *et al.* [10] studied the fluid flow across a bank of circular cylinders in pore scale for the three aforementioned porosities ($\varepsilon = 0.4345, 0.6073, 0.8076$) with Re_d up to 25. A mixed finite element method was used to discretize the partial differential equations. Instead of seeking the solution, a least square method along with a conjugated gradient algorithm was employed to approach the solution to a minimization problem. Furthermore, in their study only 49 grid points were employed for the pressure in each unit cell (i.e. 2601 points in the present computation, see Fig. 2). The use of such a methodology and coarse grid system might have led to the great understatement to the Forchheimer drag as observable from Table 1. Additional experiments are needed to resolve this dispute.

Finally, the present results of the Darcy drag (d^2/K) and the Forchheimer coefficient F are correlated by

$$\frac{d^2}{K} = \frac{31(1-\varepsilon)^{1.3}}{\varepsilon^3(\varepsilon-0.2146)} \quad (15a)$$

$$F = \frac{(1-\varepsilon)^{1.4}}{\varepsilon^3(\varepsilon-0.2146)} \sum_{n=1}^3 \sum_{m=1}^3 a_{mn} \varepsilon^{m-1} Re_d^{n-1} \quad (15b)$$

$$[a_{mn}] = \begin{bmatrix} 4.825 & -0.1660 & 0.001777 \\ -17.754 & 0.5893 & -0.006160 \\ 15.911 & -0.4736 & 0.004836 \end{bmatrix} \quad (15c)$$

They give a correlation with a maximum error of less than 5% for the Darcy–Forchheimer drag in the range of $0.2146 \leq \varepsilon \leq 1$ and $0 \leq Re_d \leq 50$.

CONCLUSION

The Darcy–Forchheimer drag is modeled numerically for a fluid flow across a bank of circular cylin-

ders. In this methodology of numerical modeling, the continuity equation and the momentum equations in pore scale are solved on a Cartesian grid system under a prescribed pressure drop. This gives rise to a numerical difficulty associated with a flow domain of irregular shape. Fortunately, the weighting function scheme along with the APPLE algorithm and the SIS solver is found quite efficient in solving such a problem. Once the velocities and the pressure distribution are known, the Darcy–Forchheimer drag is determined from the result of volumetric flow rate. The solutions verify that the viscous friction (Darcy drag) dominates the flow resistance when the granule Reynolds number is below the order of one. However, the pressure drag (the Forchheimer drag) could overtake the Darcy drag and become the dominant flow resistance at large granular Reynolds numbers. As expected, the porosity shows a great influence on the Darcy–Forchheimer drag. At its minimum possible value ($\varepsilon_{\min} = 1 - \pi/4 = 0.2146$), the flow across the cylinders even becomes theoretically impossible. Under such a situation, the Darcy–Forchheimer drag should be infinite. The present results successfully reflect this interesting phenomenon.

Acknowledgement—The authors wish to express their appreciation to the National Science Council of Taiwan for the financial support of this work through the project NSC86-2212-E007-066.

REFERENCES

- Poirier, D. R., Permeability for flow of interdendritic liquid in columnar–dendritic alloys. *Metallurgical Transactions*, 1987, **18B**, 245–255.
- Reynolds, O., *Papers on Mechanical and Physical Subjects*. Cambridge University Press, England, 1900.
- Forchheimer, P. H., Wasserbewegung durch boden. *Zeitschrift des Vereines Deutscher Ingenieure*, 1901, **45**, 1782–1788.
- Blake, F. C., The resistance of packing to fluid flow. *AIChE Journal*, 1922, **14**, 415–522.
- Ergun, S., Fluid flow through packed columns. *Chemical Engineering Progress*, 1952, **48**, 89–94.
- Macdonald, I.F., El-Sayed, M. S., Mow, K. and Dullien, F. A. L., Flow through porous media—the Ergun equa-

- tion revisited. *Industrial Engineering Chemical Fundamentals*, 1979, **18**, 199–208.
7. Ward, J. C., Turbulent flow in porous media. *Journal of Hydraulics Division, Proceedings of ASCE*, 1964, **90**, 1–12.
 8. Beavers, G. S., Sparrow, E. M. and Rodenz, D. E., Influence of bed size on the flow characteristics and porosity of randomly packed beds of spheres. *ASME Journal of Applied Mechanics*, 1973, **40**, 655–660.
 9. Beavers, G. S. and Sparrow, E. M., Non-Darcy flow through fibrous porous media. *ASME Journal of Applied Mechanics*, 1969, **36**, 711–714.
 10. Coulaud, O., Morel, P. and Caltagirone, J. P., Numerical modelling of nonlinear effects in laminar flow through a porous medium. *Journal of Fluid Mechanics*, 1988, **190**, 393–407.
 11. Lee, S. L. and Tzong, R. Y., An enthalpy formulation for phase change problems with a large thermal diffusivity jump across the interface. *International Journal of Heat and Mass Transfer*, 1991, **34**, 1491–1502.
 12. Lee, S. L. and Tzong, R. Y., Latent heat method for solidification process of a binary alloy system. *International Journal of Heat and Mass Transfer*, 1995, **38**, 1237–1247.
 13. Lee, S. L. and Tzong, R. Y., Artificial pressure for pressure-linked equation. *International Journal of Heat and Mass Transfer*, 1992, **35**, 2705–2716.
 14. Lee, S. L., A strongly implicit solver for two-dimensional elliptic differential equations. *Numerical Heat Transfer*, 1989, **16B**, 161–178.
 15. Lienhard, J. H., Synopsis of lift, drag and vortex frequency data for rigid circular cylinders. *Bulletin 300*, Washington State University, Pullman, Washington, 1966.